ELSEVIER

Journal of Biomechanics 40 (2007) 569–578

JOURNAL OF BIOMECHANICS

www.elsevier.com/locate/jbiomech
www.JBiomech.com

Stretch-induced nerve conduction deficits in guinea pig ex vivo nerve

Jianming Li, Riyi Shi*

Weldon School of Biomedical Engineering and Department of Basic Medical Sciences, School of Veterinary Medicine, Purdue University, West Lafayette, IN 47907, USA

Accepted 10 February 2006

Abstract

In the current communication, we characterized supraphysiologic elongations that elicited short-term nerve dysfunction. This was accomplished by assessing the electrophysiology of guinea pig tibial and peroneal nerves at predetermined elongation magnitudes. Results showed that a longitudinal supraphysiological stretch of $\lambda = 1.05$ caused a 16% reduction in the mean compound action potential (CAP) amplitude. Upon relaxation to physiologic length, a full recovery in the CAP was observed. At $\lambda = 1.10$, the CAP decreased by 50% with an 88% recovery after relaxation. For a supraphysiologic stretch of $\lambda = 1.20$, severe conduction block with minimal acute recovery was observed. Latency also increased during periods of stretch and was proportional to the stretch magnitude. Additional studies showed some electrophysiological recovery during the sustained stretch phase. This attribute may be related to internal stress relaxation mechanisms. Since whole nerve elongations are averaged global deformations, we also used an incremental digital image correlation (DIC) technique to characterize the strain at the micro-tissue level. The DIC analysis revealed considerable heterogeneity in the planar strain field, with some regions exhibiting strains above the macroscale stretch. This non-uniformity in the strain map arises from structural inconsistencies of the nerve and we presume that zones of high local strain may translate into the observed conduction deficits.

Keywords: Nerve; Stretch; Electrophysiology; Tension

1. Introduction

The structural characteristics of soft tissues such as muscle, ligaments and nerves have been well studied in past decades. Nerves are observed to possess viscoelastic properties (Sunderland and Bradley, 1961; Millesi et al., 1995; Kendall et al., 1979; Hartung and Arnold, 1973; Kwan et al., 1992; Driscoll et al., 2002; Ninan, 2003; Wall et al., 1991; Grewal et al., 1996) and researchers have successfully used viscoelastic theory to model individual axons and nerve tissue (Galbraith et al., 1993; Fiford and Bilston, 2005; Ninan, 2003). The combined biomechanical data demonstrate that at small loads, the nerve is quite compliant, exhibiting high strains while incurring minimal stresses. Morphologically, elevated strains will cause the axons and surrounding connective tissue to reorient in the direction of load. This reorientation process is manifested in the "toe" region of the stress–strain profile and is followed by transition into a stiffer, linear zone (Rydevik et al., 1990).

In terms of functional consequences, there have been numerous clinical and experimental studies investigating the stretch injury limit of nervous tissue. Values ranging from 25% (Mitchell, 1872; Hoen and Brackett, 1956) to 100% strain (Denny-Brown and Doherty, 1945) have been reported. More recently, Haftek (1970) and Rydevik et al. (1990) tracked the nerve morphological response to tension, demonstrating axonal disorganization and connective tissue rupture at strains beyond the elastic limit. Still others have used in vivo models to gauge the electrophysiology during elevated states of

*Corresponding author. Tel.: +1 765 496 3018; fax: +1 765 494 7605.
E-mail address: riyi@purdue.edu (R. Shi).

0021-9290/$ - see front matter © 2006 Elsevier Ltd. All rights reserved.
doi:10.1016/j.jbiomech.2006.02.009

tension or stretch (Takai et al., 2002; Bain and Meaney, 2000; Jou et al., 2000; Wall et al., 1992; Kwan et al., 1992). Collectively, the results from the morphological and electrophysiological studies have been conflicting and inconsistent. Part of the discrepancy can be attributed to testing methodology, specimen-to-specimen variations, measured endpoints and the challenging nature of nerve testing. However, it is widely agreed that supraphysiologic mechanical loads do cause functional deficit. Thus, the objective of this study was to quantify and elucidate the physiological response of nerves to simple elongation. Our methodology involved exposing guinea pig tibial and peroneal nerves to sustained supraphysiologic elongations of $\lambda = 1.05$, 1.10 and 1.20 while simultaneously monitoring whole nerve electrophysiology. To further understand the nature of stretch injuries, we also performed trials where longer stretch durations of 5 and 10 min were used. The stretch at the macroscale level was then correlated to micro level strains via digital image correlation (DIC) methods. Application of the imaging correlation algorithms allowed us to gain a more meaningful insight into the strain distribution of the model system.

2. Materials and methods

2.1. Nerve isolation and in vivo elongation measurement

All animals used in this study were handled in strict accordance with the National Institutes of Health guide for the Care and Use of Laboratory Animals and the experimental protocol was approved by the Purdue Animal Care and Usage Committee.

Adult female guinea pigs (325–500 g) were anesthetized using ketamine (80 mg/kg) and xylazine (12 mg/kg) and perfused with oxygenated 15 °C Kreb's buffer solution to remove blood and lower core body temperature. The guinea pigs were placed dorsal side up on a stainless steel grate. An incision was made in the hamstring muscle to reveal the sciatic nerve. The hind legs were then flexed such that the hip joint, knee joint and ankle (toes extended) were collinear along a 45° angle within a plane parallel to the grate surface (Fig. 1A and B). Next, a pair of dye marks 12 mm apart was made on the sciatic nerve. This gauge length (L_0) corresponded to an estimated state of maximum physiologic stretch, as constrained by kinematics and anatomy (Fig. 1B). After excision, the sciatic nerve (4–5 cm) was allowed to fully retract in a 15 °C oxygenated (95%O_2, 5% CO_2) Kreb's solution for 5 min. After 5 min, the retracted dye distance (L_R, Fig. 1C) was measured with calipers (± 0.01 mm). The in vivo elongation was estimated as L_0/L_R with L_R being the retracted nerve gauge length. The sciatic nerve was then split with a #12 surgical blade to isolate the tibial and peroneal component (following the natural peroneal/tibial demarcation). All extraneous connective tissue was removed. The nerves were re-incubated in the oxygenated Kreb's solution for approximately 1 h to recover from the surgical process.

2.2. Experimental setup and electrophysiological recording

An illustration of the isolation chamber (modified from Shi and Blight, 1996; Ninan, 2003) and experimental setup is shown in Fig. 2A. After the 1 h incubation period, nerves were randomly placed (distal left, proximal right or vice versa) into the isolation chamber. The resting nerve was fixed at one end while the other end was clamped to a digital force transducer (Mark-10). The force transducer was in turn mounted to a motorized micromanipulator (Newport). Next, viscous silicone grease (Dow Corning) was placed into the machined grease wells. Care was taken to ensure sound grease barriers. The micromanipulator was then displaced such that the dye marks on the nerve corresponded to the gauge length, L_0 (Fig. 1B). This length was considered the new baseline level for supraphysiologic elongations. Isotonic KCl solution was subsequently pipetted into the end wells and oxygenated Kreb's solution filled the center well. A transparent cover plate was also placed over the chamber to seal the wells. A gas inlet tube was then inserted into an opening in the central well and a 95% O_2/5% CO_2 gas mixture was fed into this tube to aerate the buffer solution. Electrophysiology testing was commenced after the nerve had several minutes to equilibrate and the CAP waveform had reached steady state. At this point, the micromanipulator clamp was translated at a rate of 0.079 mm/s to the appropriate elongation magnitude and held for either 2.5, 5 or 10 min. The supraphysiologic stretch ratio (longitudinal) was calculated as $\lambda = L'/L$, where L was taken as the clamp to clamp nerve length and L' was the stretched clamp to clamp nerve length. After the sustained stretch phase, the nerve was allowed to return to length L at the same 0.079 mm/s clamp speed. Ag/AgCl electrodes were used to stimulate (supramaximal intensity) and measure the electrophysiology. Recordings were made using a bridge amplifier (Neurodata Instruments) and data analysis performed using custom Labview software (National Instruments) on a PC. Instantaneous waveforms and time histories were recorded and digitized. The nerve was maintained at temperatures in the range of 22–25 °C. Prior studies using this chamber apparatus showed stable action potentials for well over 60 min. To prevent confounding and pre-conditioning effects, nerve specimens were only stretched once.

2.3. Measured electrophysiological parameters

The endpoints of our functional assessment included compound action potentials (CAP), latency and changes

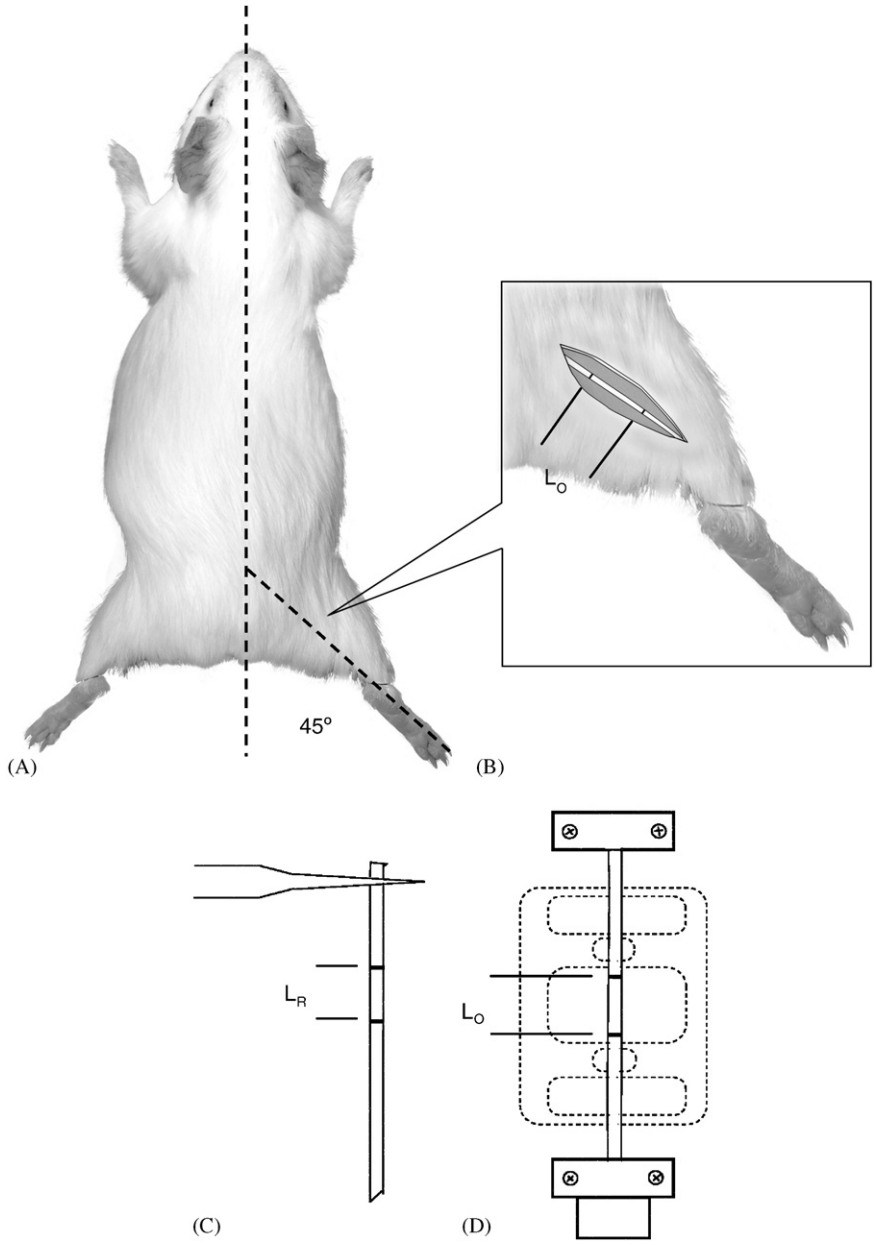

Fig. 1. (A) Drawing describing the positioning of the guinea pig during the nerve excision process. The guinea pig was placed dorsal side up on a metal platform with the hip joint, knee joint and ankle joint (toes extended) collinear along a 45° angle with respect to the body (in a plane parallel to the platform). (B) A pair of dye marks 12 mm apart was made on the sciatic nerve. This gauge length (L_0), corresponds to an estimated maximum physiologic stretch state as constrained by joint kinematics and anatomy. (C) After excision, the sciatic nerve was allowed to fully retract (L_R), and the ratio of L_0/L_R calculated to approximate the maximum in vivo stretch. (D) Prior to electrophysiology, the nerves were stretched such that the dye marks distance equaled the L_0 gauge length (see Fig. 2A for complete electrophysiology setup). Then, stretch of $\lambda = 1.00$ (control), $\lambda = 1.05$, 1.10 and 1.20 beyond L_0 (supraphysiologic) were performed concurrently with the electrophysiology. All nerves were used once and were not intentionally preconditioned prior to experimental testing.

in the compound membrane potential. The CAP is defined as the sum of all evoked action potentials. Consistent with multi-unit recordings, the composite CAP waveform is believed to be dominated by larger caliber axons (Jensen and Shi, 2003). Contributions from slower, smaller fibers are minor and would tend to aggregate at the tail end of the CAP waveform. Further, since the peroneal and tibial nerves are mixed nerves, both motor and sensory pathways are recorded. Typical CAP amplitudes ranged from 1–6 mV and were not a function of nerve type (peroneal/tibial). Decreases in the CAP amplitude would commonly convey loss of electrical function. The acquired CAP waveforms also gave latency (time from stimulus to CAP peak) data. In addition, we were also able to assess the compound resting membrane potential (gap potential). The gap

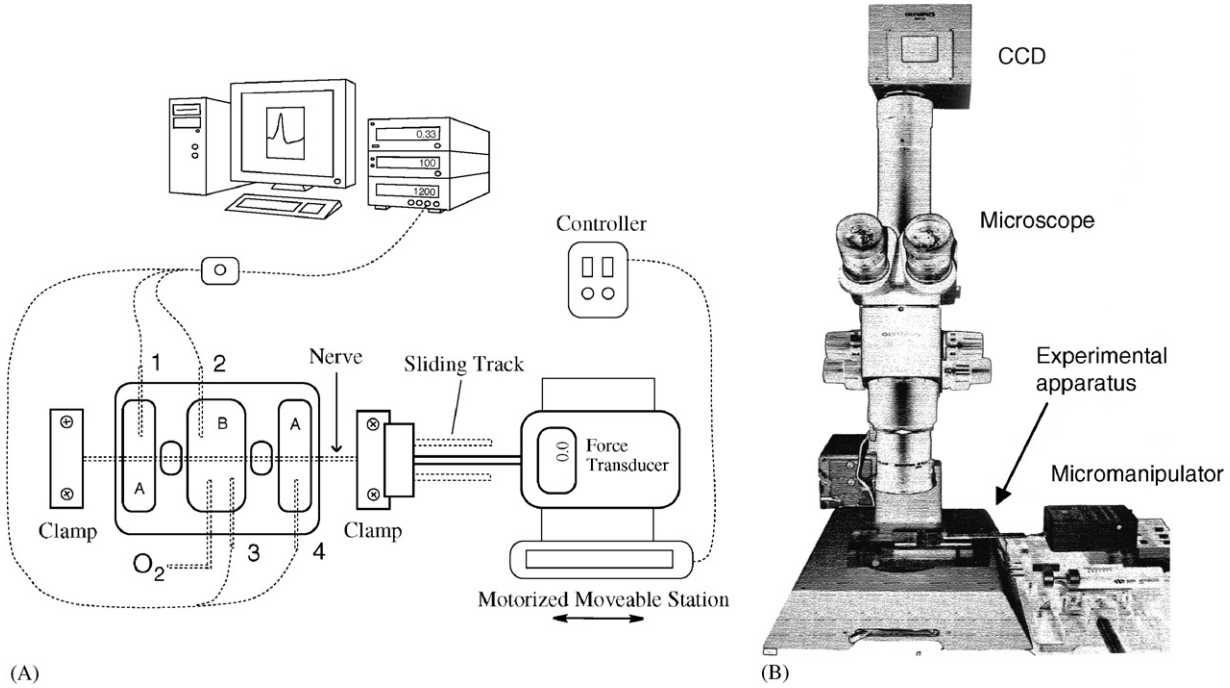

Fig. 2. (A) Schematics of the tissue isolation chamber and experimental setup. Designations: 1, 2—recording electrode pair, 3, 4—stimulating electrode pair, *A*—isotonic (120 mM) potassium chloride, B—Oxygenated Kreb's solution. The nerve resided in the middle of the chamber and was clamped (using cyanoacrylate glue and texturized rubber pads) to a stationary mount and a moveable clamp. The moveable clamp was attached to a force transducer (Mark-10) and the force transducer rested on a micromanipulator. During stretch, the translating clamp was moved at speeds of 0.079 mm/s (controller). Omitted in the diagram was the cover for the chamber that aided in preserving the gaseous environment. The electrophysiological setup composed of a Grass stimulator and a data recording unit (Neurodata). Nerves were stimulated above threshold intensities at 0.33 Hz. (B) Configuration for determination of the strain field during stretch. Nerves were placed in the chamber and viewed under an Olympus SZX-12 microscope. Ink drops were airbrushed onto the nerve to form a speckle pattern and a DP-10 CCD recorded the serial brightfield images at designated stretch magnitudes. The digital images were subsequently analyzed with an image correlation program (Roeder et al., 2004).

potential is a parameter that describes membrane ionic permeability and serves as an indicator of membrane integrity (Shi et al., 2000).

2.4. Correlation of elongation to tissue level strain

To quantify the strain at the micro level during elongation, Lagrangian strains were separately assessed by tracking localized tissue deformations. Excised nerves were placed in the electrophysiological recording apparatus that was arranged under an Olympus SZX-12 microscope (Fig. 2B). The nerves were then stretched to estimated maximum physiologic lengths. An airbrush was used to apply micron sized ink droplets onto the nerve. An Olympus DP10 CCD recorded serial brightfield images of the nerve at nerve positions corresponding to the maximum physiologic length and successive supraphysiologic stretch of $\lambda = 1.05$, 1.10 and 1.20. The 1280×1024 pixel size images were then converted to grayscale. To calculate the strain field, we employed DIC methods and used an algorithm previously described by Roeder et al. (2004). Briefly, the DIC algorithm follows the ink intensity pattern (displacement field) and outputs the 2-D Lagrangian strain map. Accuracy of computer analyses was verified with multiple hand calculations.

2.5. Statistical analysis

All reported electrophysiology data is in the form of mean $\pm$ standard deviation. For CAP and latency data, the non-parametric Kruskal–Wallis test was employed and a post-hoc Dunn's test was used to compare the experimental treatments to their respective control groups. A p-value of less than 0.05 was considered to be statistically significant.

3. Results

3.1. Physiologic elongations

Measurements of the guinea pig sciatic nerve at a limb-extended state were made in an attempt to approximate stretch values generally found within the in vivo environment. When the hind limb was held at the predetermined bodily position, the striations of Fontana were not observed. This suggests the nerves

Table 1
Summary of electrophysiology

λ	Stretch duration (min)	Initial CAP	CAP during stretch	Recovered CAP	Initial latency	Latency during stretch	Recovered latency
1.00	2.5	1.000	0.985 ± 0.029 ($n=10$)	0.977 ± 0.033 ($n=10$)	1.000	1.022 ± 0.025 ($n=8$)	1.048 ± 0.045 ($n=8$)
1.05	2.5	1.000	$0.836\pm0.078^{*}$ ($n=10$)	0.966 ± 0.046 ($n=10$)	1.000	1.182 ± 0.369 ($n=9$)	1.169 ± 0.255 ($n=9$)
1.10	2.5	1.000	$0.500\pm0.086^{**}$ ($n=14$)	$0.884\pm0.109^{*}$ ($n=14$)	1.000	$1.527\pm0.475^{**}$ ($n=14$)	$1.308\pm0.269^{*}$ ($n=14$)
1.10	5	1.000	$0.532\pm0.108^{**}$ ($n=6$)	0.969 ± 0.083 ($n=6$)	1.000	1.231 ± 0.323 ($n=5$)	1.102 ± 0.139 ($n=5$)
1.10	10	1.000	$0.467\pm0.090^{**}$ ($n=5$)	$0.895\pm0.054^{**}$ ($n=5$)	1.000	1.324 ± 0.358 ($n=4$)	1.339 ± 0.376 ($n=4$)
1.20	2.5	1.000	$0.054\pm0.076^{**}$ ($n=10$)	$0.080\pm0.114^{**}$ ($n=10$)	1.000	–	–

All data reported are normalized with respect to initial readings. Values are in the form of mean $\pm$ SD.
$^{*}p<0.05$.
$^{**}p<0.01$.

had become uncoiled from their unstressed wavy disposition (Pourmand et al., 1994; Sunderland, 1990). With the limb extended, the ratio of L_0/L_R was determined to be 1.097 ± 0.020 ($n=37$). We conclude that during in vivo conditions, the nerve gauge length will experience stretch below this magnitude. This assumption was made based on observing the hind limb joint kinematics. Electrophysiology at elongations beyond the perceived limit was then performed to ascertain the conduction response of supraphysiologic stretch.

3.2. Electrophysiology of nerves under stretch

All concomitant electrophysiology-elongation data is summarized in Table 1. The electrophysiological records revealed conduction deficits were immediate beyond physiologic elongations (Fig. 3). At a supraphysiologic stretch of $\lambda=1.05$, the normalized mean CAP decreased to 0.836 ± 0.078. Insignificant changes in latency were observed at this level of injury. A full recovery in the CAP (0.966 ± 0.046) was seen post-stretch when compared to control samples. At $\lambda=1.10$, the CAP decreased to 0.500 ± 0.086 while the latency climbed to 1.527 ± 0.475. Removal of stretch caused a return of the CAP amplitude close to pre-injury limits (0.884 ± 0.109), where as recovered latency was significantly longer compared to the initial uninjured state (1.308 ± 0.269). Electrophysiological recovery was quick, with steady-state conditions attained within 15 min post trauma. For $\lambda=1.20$, there was essentially full conduction block with the majority of the specimens remaining non-conducting 30 min after injury. Latency for non-functional stretch damaged nerves could not be calculated. The compound membrane potential did not fluctuate at any stretch magnitudes tested (data not shown). Typical instantaneous CAP waveforms are shown in Fig. 3B. Macroscopically, the nerve was intact in all test samples and no plastic deformation was seen. However, at $\lambda=1.20$, the structural recovery back to the L_0 gauge length was consistently prolonged. This observation is characteristic of viscoelastic materials, which commonly show a delayed memory effect (Fung, 1981; Flugge, 1975).

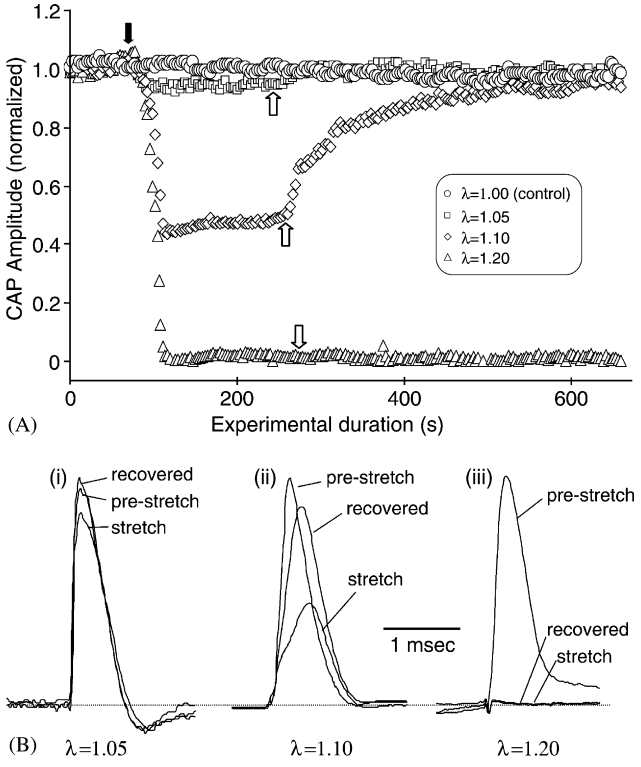

Fig. 3. (A) Representative CAP amplitude time histories for $\lambda=1.00$, 1.05, 10 and 1.20. The filled arrows mark the commencement of stretch whereas the open arrows depict the start of clamp relaxation. The clamp crosshead velocity used was 0.079 mm/s in all cases, which approximated to a strain rate of 0.003/s. (B) Typical waveforms for $\lambda=1.05$, 1.10 and 1.20 are shown. With $\lambda=1.05$ (i), there was a slight drop in the CAP amplitude during stretch, with statistically insignificant changes in latency. Relaxation of the nerve induced a full reversion of conduction deficit. In the $\lambda=1.10$ case (ii), the CAP was drastically altered in conjunction with longer latency values. Removal of traction saw a recovery of the CAP and latency. Full conduction block at $\lambda=1.20$ (iii) was seen in most instances. After removal of elongation, there was minimal improvement in the electrophysiology even after 30 min.

3.3. Prolonged elongation times

When subjected to longer elongation durations ($\lambda = 1.10$, stretch held for 5 or 10 min), the CAP demonstrated a behavior similar to nerves stretched for 2.5 min (Fig. 4A, Table 1). For 5 min stretch injury trials, the CAP decreased to 0.532 ± 0.108 while the 10 min held samples showed a reduction to 0.467 ± 0.090 (values at the onset of sustained stretch). Latency for the stretch and recovery phases were not statistically significant compared to respective controls. During the sustained stretch period, the CAP amplitude increased slightly (~5–10%) in most cases. This recovery event coincided with the stress relaxation of the nerve (Fig. 4B). The longer elongation times did not seem to inhibit the final CAP recovery response. Both 5 and 10 min stretch samples showed CAP improvement that approached pre-injured levels, although the rate of recovery was typically slower than those specimens stretched for only 2.5 min (Fig. 4C). Similar to 2.5 min trials, whole nerve structural continuity was preserved in both 5 and 10 min stretched specimens.

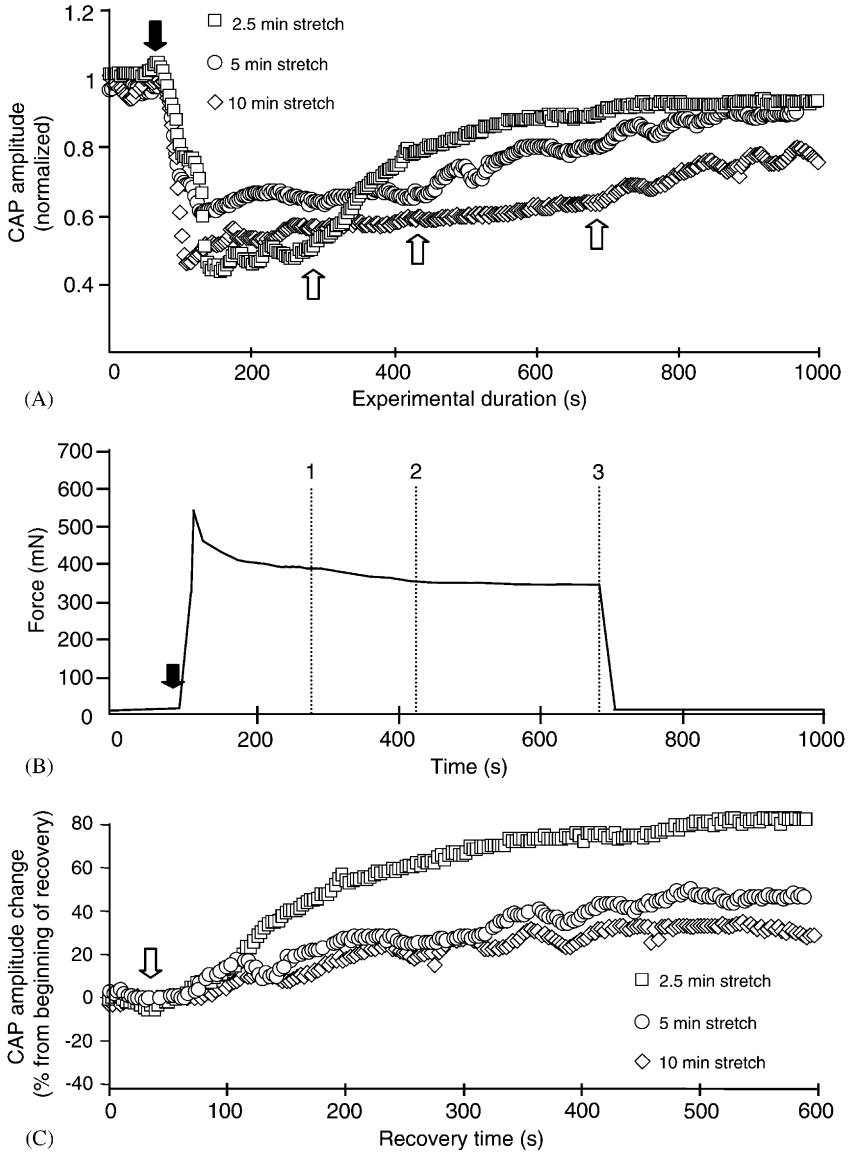

Fig. 4. (A) Typical time histories of nerve specimens subjected to elongation times of 2.5, 5 and 10 min ($\lambda = 1.10$). Filled and open arrows mark the beginning and end of stretch, respectively. During the sustained stretch phase, noticeable recovery in CAP amplitudes was noted. (B) Characteristic load-time curve obtained from the force transducer. The load decay depicts the nerve stress relaxation phenomenon and corresponds well to the CAP recovery event. Filled arrow marks the stretch event and dashed lines 1, 2 and 3 denote the ensuing 2.5, 5 and 10 min. In this example, the stretch was sustained for 10 min. (C) To evaluate the effects of elongation times on CAP recovery rate, plots from Fig. 4(A) were time translated to correspond to the same recovery reference point. Open arrow indicates release of traction. Note the slower upstroke (slope) of CAP response in the prolonged stretch specimens.

3.4. Correlation between elongation and tissue level strain

The DIC technique was applied to portions of the nerve relevant to electrophysiology (i.e. middle and end wells). Typical strain maps produced from the DIC algorithm are depicted in Fig. 5. It is apparent that even within the same nerve, the strains varied considerably as a function of location. For each nerve tested, the minimum Lagrangian strain ($E_{11-\min}$), the average strain ($\bar{E}_{11}$) and the maximum strain ($E_{11-\max}$) were tabulated. The collective data for each strain measure was then plotted for every level of stretch (Fig. 6). For comparison, we further calculated the theoretical $\bar{E}_{11}$ (at each level of λ) for a homogeneous nerve in the absence of clamp stress concentrations (Fig. 6). This theoretical $\bar{E}_{11}$ was found by using the relation: $\bar{E}_{11} = \frac{1}{2}(\lambda^2 - 1)$. Results for the experimental $\bar{E}_{11}$ ($\pm$S.D., $n = 14$) were observed to be 0.042 ± 0.025, 0.074 ± 0.026 and 0.137 ± 0.041 for $\lambda = 1.05, 1.10, 1.20$, respectively. These values of $\bar{E}_{11}$ were considerably lower than predicted and suggest the clamp stress concentrations have a significant impact in defining the strain intensity pattern. In contrast, the averaged peak strain magnitudes were found to be 0.060 ± 0.031, 0.117 ± 0.053 and 0.183 ± 0.083 for $\lambda = 1.05, 1.10, 1.20$, respectively. These magnitudes were comparable to the theoretical $\bar{E}_{11}$ in a homogeneous nerve.

The DIC method was also able to compute the lateral (E_{22}) and shear strains (E_{12}). As expected, E_{22} concentrations were co-localized with E_{11} maximums (Poisson

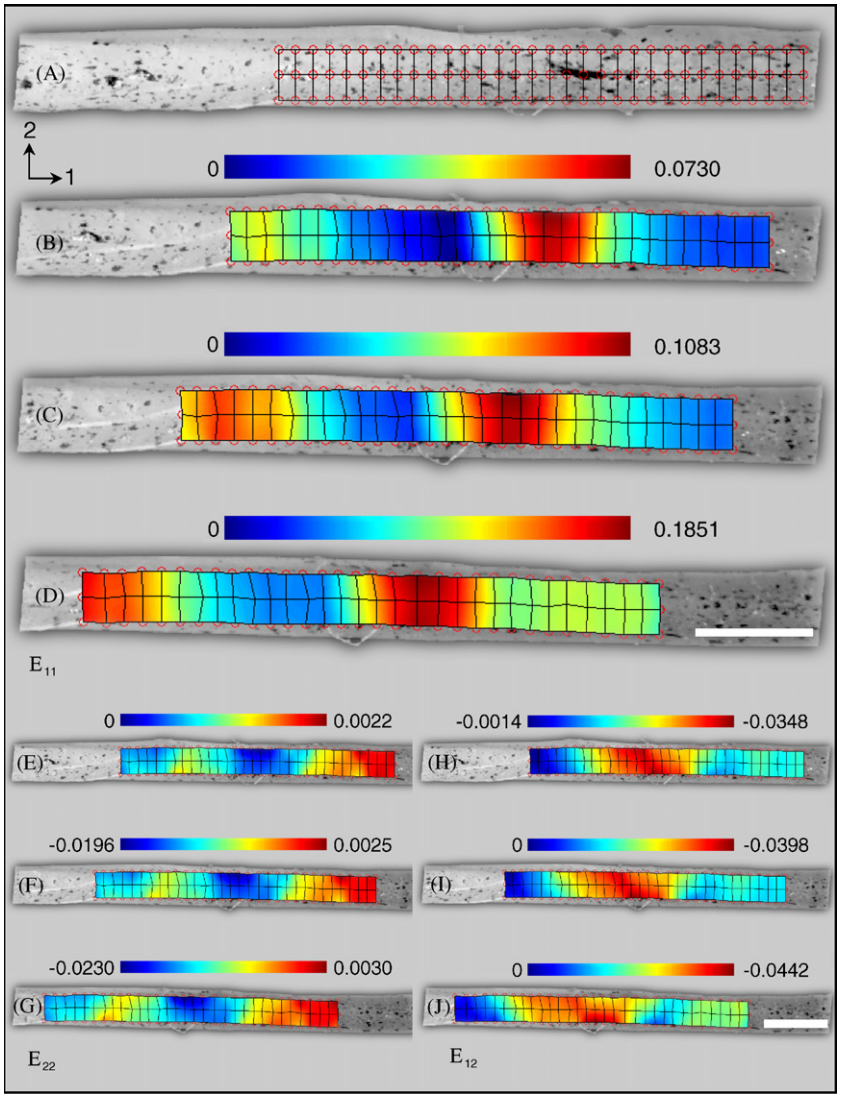

Fig. 5. An experimental DIC output for a sample nerve is shown. (A) Initial image depicting the nerve at maximum physiologic elongation. Prescribed points were then superimposed onto the nerve to outline the undeformed areal elements. The longitudinal strain (E_{11}) map corresponding to supraphysiologic stretch of $\lambda = 1.05$ (B), $\lambda = 1.10$ (C) and $\lambda = 1.20$ (D) were then calculated. Note the heterogeneity in the strain field, including regions of high and low strain. Companion outputs for the lateral strain (E_{22}) were also plotted for stretch ratios of $\lambda = 1.05$ (E), $\lambda = 1.10$ (F) and $\lambda = 1.20$ (G). Likewise, the shear strain (E_{12}) was also determined for $\lambda = 1.05$ (H), $\lambda = 1.10$ (I) and $\lambda = 1.20$ (J). As expected, the E_{22} strains were co-localized with E_{11} strains due to the Poisson effect. Scale bar: 1 mm (A–D), 1 mm (E–J).

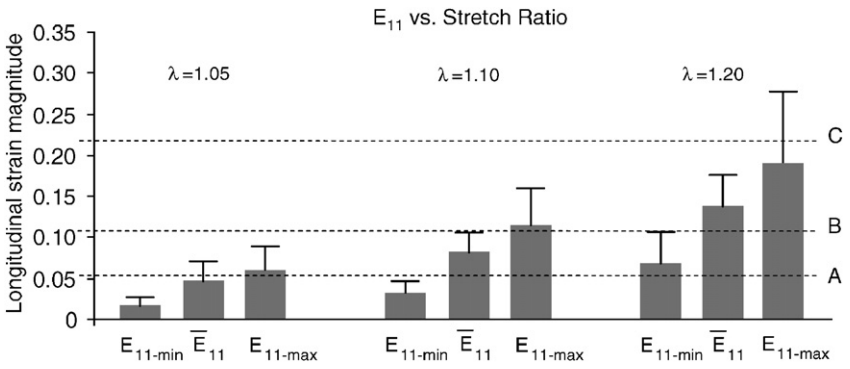

Fig. 6. Values for minimum strain ($E_{11-\min}$), average strain ($\bar{E}_{11}$) and maximum strain ($E_{11-\max}$) were tabulated to assess the trend between the applied macroscale stretch and the actual tissue level strains. The averaged results for each parameter were as follows ($\lambda = 1.05$, 1.10 and 1.20, respectively): $E_{11\min}$: 0.015 ± 0.011, 0.036 ± 0.017, 0.066 ± 0.045; $\bar{E}_{11}$: 0.042 ± 0.027, 0.074 ± 0.030, 0.137 ± 0.042; $E_{11\max}$: 0.060 ± 0.031, 0.117 ± 0.053, 0.183 ± 0.087. For comparison, dashed lines A, B and C denote the expected E_{11} in a homogeneous nerve (and ignoring clamp concentrations) with uniform strain.

effect). However, we are uncertain what roles the lateral and shear strains play in shaping axonal injury. The lateral and shear strains were also relatively small compared to the longitudinal component. We therefore presume the observed conduction deficits to be primarily caused by strain in the longitudinal direction and statistical data for E_{22} and E_{12} were not reported.

4. Discussion

Characterizing the thresholds for nerve dysfunction under stretch is a topic of considerable interest in clinical and modeling applications. Seminal studies pertaining to stretch tolerances in mammals have produced wide-ranging data, with strain limits of 25–100% being reported (Mitchell, 1872; Denny-Brown and Doherty, 1945). More recently, Kwan et al. (1992) showed that a 6% strain in rabbit tibial nerves reduced the CAP by 40% after 1 h of sustained stretch. Removal of traction fully restored the CAP. At 12% strain, the CAP was extinct at 1 h with only 40% recovery post-trauma. On the other hand, Takai et al. (2002) reported that an 8.1% in situ strain caused complete conduction block when using rabbit brachial plexus nerves and compound muscle action potential (CMAP) recordings (Takai et al., 2002). Upon relaxation, the CMAP recovered to 92% of control levels within 10 min. Jou et al. (2000) showed that rat femoral lengthening beyond 8% caused deficits in the sciatic nerve while Bain and Meaney (2000) found electrophysiological strain thresholds between 0.09 and 0.47 for the guinea pig optic nerve model.

However, comparing quantitative data between studies is problematic. First, we recognize that species and tissue variations exist and we are uncertain how well our data translates to other animal or human models. Even within the same species, nerve structure varies by location. For instance, the guinea pig optic nerve appears to be more homogeneous than the sciatic nerve (Bain and Meaney, 2000; Fine and Yanoff, 1979). These structural differences may dictate the severity of damage. A homogeneous structure would create a more diffuse injury pattern while heterogeneous tissue would produce strain concentrations and more localized lesions. Secondly, how the stretch was applied and measured must be considered as that may be a source of confusion (i.e. averaged global deformations vs. local tissue strains).

Finally, there remains the discrepancy between in vivo and ex vivo preparations. In sustained in vivo studies, it is not possible to completely decouple mechanical damage from ischemic injury. For example, Lundborg and Rydevik (1973) found that an 8% stretch caused blood flow to decrease by 50% in rabbit tibial nerves. Similar results were corroborated with rabbit sciatic nerve (Ogata and Naito, 1986). In vivo studies may therefore, have a component of damage associated with the hemodynamic response. With ex vivo preparations, mechanical injury can be isolated from the confounding ischemia (Ochs et al., 2000; Shi and Blight, 1996; Shi and Pryor, 2002).

In the current communication, we probed the effects of sustained elongation on whole nerve electrophysiology. A relationship between elongation magnitudes and the degree of conduction dysfunction was demonstrated in the context of an ex vivo model (Table 1). Correlation of the macroscale elongations to 2-D Lagrangian strains emphasized the disparity that can exist between the global and local level deformations. The magnitude and heterogeneity of the strain pattern also present a number of intriguing insights. In some situations, high strains expectedly coincided with regions of smaller nerve diameter. In other instances, extreme strains occurred quite "randomly" and did not correspond to localized geometric irregularities. We surmise the differing strain

zones to be partly caused by heterogeneity in the mechanical properties along the nerve. It was previously observed with rat sciatic nerve that joint regions encountered strains 5–10 times higher than non-joint sections (Phillips et al., 2004). Further histological data did not ascribe these discrepancies to degree of fasciculation. Currently, we have not studied whether strain concentrations co-localized with joint regions but this phenomenon as well as micro-level deviations (within joint/non-joint segments) in the mechanical properties could exist. These extremes in mechanical properties would dictate the resultant strain field and potentially predispose compliant region(s) to unusually high levels of strain. Since it has been suggested that high regional strains may coincide with white matter damage (Fiford et al., 2004; Blight and Decrescito, 1986), it is evident how even small global elongations can induce measurable conduction deficit. Our experimental injury data suggest that nerves respond to supraphysiologic elongations as small as $\lambda = 1.05$ while stretch of $\lambda = 1.10$ or greater may be detrimental from a recovery standpoint.

The conduction behavior of nerves subjected to longer elongation times was noteworthy. During sustained stretch, the CAP amplitude (but not latency) increased by approximately 5–10%. We were intrigued how this CAP improvement paralleled the viscoelastic stress relaxation effect. It may be possible that the reorientation of yet undetermined internal elements during relaxation could ameliorate conduction deficit. An alternative hypothesis that has been proposed describes a state of increased membrane/nodal excitability initiated by stretch (Ochs et al., 2000; Tanelian and Markin, 1997). This explanation could lead to the increased CAP signals. The relaxation event may also explain the retarded recovery times of 5 and 10 min experiments (Fig. 4) as the advanced state of internal reorganization brought on by the extra stretch period could pose a barrier to functional recovery. However, the longer stretch durations did not hinder final recovery outcomes (0.969 ± 0.083 and 0.895 ± 0.054 for 5 and 10 min, respectively). Interestingly, in vivo studies in which the nerve stress was maintained constant demonstrated a progressive CAP deterioration (Kwan et al., 1992). Thus, there appears to be differences in the electrophysiology when either a creep or stress relaxation paradigm is used.

The current experimental model does not explain the mechanistics of the mechanical injury but possibilities that have been proposed include transient changes in membrane ion channel conformation, a damaged membrane, myelin disruption or an increase in axial resistivity that diminishes ionic currents (Haftek, 1970; Galbraith et al., 1993; Ochs et al., 2000). We speculate from our compound membrane potential data that the membrane was not compromised, even at 20% stretch. This finding is consistent with Galbraith et al. (1993), who used single giant squid axons in an in vitro model. They discovered that at small elongations (<19%) and slow stretch rates (0.284 mm/s), effects on membrane potential were negligible. Subsequent studies by Smith et al. (1999) also showed that the permeability of the axon membrane is unchanged at strains of up to 60% in human NT2 cells. Although we hypothesize membrane damage to be improbable, the present study does not support or preclude other explanatory possibilities such as an altered ion channel state or increased axonal resistivity.

We presently addressed quasi-static (0.003/s) elongation but it may be constructive to conduct higher strain rate evaluations in the future. Dynamic stretch data may be more applicable to traumatic injury situations, which typically occur at higher strain rates. Although rate loading data with gross peripheral nerve is limited, evidence with organotypic brain slices suggests strain rate to be a critical factor in dictating expression of cell survival and cell death genes (Morrison et al., 2000). Higher rates of loading have also been demonstrated to increase membrane permeability or tissue damage with cellular models and in spinal cord preparations (Galbraith et al., 1993; LaPlaca et al., 1997; Lusardi et al., 2004; Jensen and Shi, 2003; Fiford et al., 2004). Nonetheless, the present quasi-static study on peripheral nerves is relevant by elucidating the levels of sustained elongation that cause acute conduction block. This data could shed light on the etiology of repetitive strain injuries (Julius et al., 2004), setting thresholds for nerve repair or computational modeling and in developing mechanically matched tissue constructs.

Acknowledgments

We would like to acknowledge Dr. Sherry Voytik-Harbin, Dr. Blayne Roeder and Brett Bell for their generous assistance in implementing the DIC technique. We would also like to thank Phyllis Zickmund and Dr. Jennifer McBride for their aid with tissue preparation. This research was funded by the NSF Integrative Graduate Education and Research Training (IGERT) Program in Therapeutic and Diagnostic Devices DGE-99-72770 and the State of Indiana.

References

Bain, A.C., Meaney, D.F., 2000. Tissue-level thresholds for axonal damage in an experimental model of central nervous system white matter injury. Journal of Biomechanical Engineering 122, 615–622.

Blight, A.R., Decrescito, V., 1986. Morphometric analysis of experimental spinal cord injury in the cat: the relation of injury intensity to survival of myelinated axons. Neuroscience 19, 321–341.

Denny-Brown, D., Doherty, M.M., 1945. Effects of transient stretching of peripheral nerve. Archives of Neurology and Psychiatry 54, 116–129.

Driscoll, P.J., Glasby, M.A., Lawson, G.M., 2002. An in vivo study of peripheral nerves in continuity: biomechanical and physiological responses to elongation. Journal of Orthopaedic Research 20, 370–375.

Fiford, R.J., Bilston, L.E., 2005. The mechanical properties of rat spinal cord in vitro. Journal of Biomechanics 38, 1509–1515.

Fiford, R.J., Bilston, L.E., Waite, P., Lu, J., 2004. A vertebral dislocation model of spinal cord injury in rats. Journal of Neurotrauma 21, 451–458.

Fine, B., Yanoff, M., 1979. Ocular Histology, second ed. Harper and Row, New York.

Flugge, W., 1975. Viscoelasticity. Springer, Berlin.

Fung, Y.C., 1981. Biomechanics: Mechanical Properties of Living Tissue. Springer, New York.

Galbraith, J.A., Thibault, L.E., Matteson, D.R., 1993. Mechanical and electrical responses of the squid giant axon to simple elongation. Journal of Biomechanical Engineering 115, 13–22.

Grewal, R., Xu, J., Sotereanos, D.G., Woo, S.L., 1996. Biomechanical properties of peripheral nerves. Hand Clinics 12, 195–204.

Haftek, J., 1970. Stretch injury of peripheral nerve. Acute effects of stretching on rabbit nerve. Journal of Bone and Joint Surgery-British 52, 354–365.

Hartung, C., Arnold, G., 1973. Histomechanical properties of peripheral nerves. Nervenarzt 44, 80–84.

Hoen, T.I., Brackett, C.E., 1956. Peripheral nerve lengthening. I. Experimental Journal of Neurosurgery 13, 43–48.

Jensen, J.M., Shi, R., 2003. Effects of 4-aminopyridine on stretched mammalian spinal cord: the role of potassium channels in axonal conduction. Journal of Neurophysiology 90, 2334–2340.

Jou, I.M., Lai, K.A., Shen, C.L., Yamano, Y., 2000. Changes in conduction, blood flow, histology, and neurological status following acute nerve-stretch injury induced by femoral lengthening. Journal of Orthopaedic Research 18, 149–155.

Julius, A., Lees, R., Dilley, A., Lynn, B., 2004. Shoulder posture and median nerve sliding. BMC Musculoskeletal Disorder 23, 1–7.

Kendall, J.P., Stokes, I.A., O Hara, J.P., Dickson, R.A., 1979. Tension and creep phenomena in peripheral nerve. Acta Orthopaedica Scandinavica 50, 721–725.

Kwan, M.K., Wall, E.J., Massie, J., Garfin, S.R., 1992. Strain, stress and stretch of peripheral nerve. Rabbit experiments ex vivo and in vivo. Acta Orthopaedica Scandinavica 63, 267–272.

LaPlaca, M.C., Lee, V.M., Thibault, L.E., 1997. An in vitro model of traumatic neuronal injury: loading rate-dependent changes in acute cytosolic calcium and lactate dehydrogenase release. Journal of Neurotrauma 14, 355–368.

Lundborg, G., Rydevik, B., 1973. Effects of stretching the tibial nerve of the rabbit: a preliminary study of the intraneural circulation and the barrier function of the perineurium. Journal of Bone and Joint Surgery 55-B, 390–401.

Lusardi, T.A., Wolf, J.A., Putt, M.E., Smith, D.H., Meaney, D.F., 2004. Effect of acute calcium influx after mechanical stretch injury in vitro on the viability of hippocampal neurons. Journal of Neurotrauma 21, 61–72.

Millesi, H., Zoch, G., Reihsner, R., 1995. Mechanical properties of peripheral nerves. Clinical Orthopaedics and Related Research 314, 76–83.

Mitchell, S.W., 1872. Injury of Nerves and Their Consequences. Lippincott, Philadelphia.

Morrison III., B., Meaney, D.F., Margulies, S.S., McIntosh, T.K., 2000. Dynamic mechanical stretch of organotypic brain slice cultures induces differential genomic expression: relationship to mechanical parameters. Journal of Biomechanical Engineering 122, 224–230.

Ninan, L., 2003. Study of nerve failure and the repair of nerves using synthetic and biological polymers. Ph.D. Thesis, Purdue University, West Lafayette.

Ochs, S., Pourmand, R., Si, K., Friedman, R.N., 2000. Stretch of mammalian nerve in vitro: effect on compound action potentials. Journal of the Peripheral Nervous System 5, 227–235.

Ogata, K., Naito, M., 1986. Blood flow of peripheral nerve effects of dissection, stretching and compression. Journal of Hand Surgery 11, 10–14.

Phillips, J.B., Smit, X., De Zoysa, N., Afoke, A., Brown, R.A., 2004. Peripheral nerves in the rat exhibit localized heterogeneity of tensile properties during limb movement. Journal of Physiology 557, 879–887.

Pourmand, R., Ochs, S., Jersild Jr., R.A., 1994. The relation of the beading of myelinated nerve fibers to the bands of Fontana. Neuroscience 61, 373–380.

Roeder, B.A., Kokini, K., Robinson, J.P., Voytik-Harbin, S.L., 2004. Local, three-dimensional strain measurements within largely deformed extracellular matrix constructs. Journal of Biomechanical Engineering 126, 699–708.

Rydevik, B.L., Kwan, M.K., Myers, R.R., Brown, R.A., Triggs, K.J., Woo, S.L., Garfin, S.R., 1990. An ex vivo mechanical and histological study of acute stretching on rabbit tibial nerve. Journal of Orthopaedic Research 8, 694–701.

Shi, R., Blight, A.R., 1996. Compression injury of mammalian spinal cord in vitro and the dynamics of action potential conduction failure. Journal of Neurophysiology 76, 1572–1580.

Shi, R., Pryor, J.D., 2002. Pathological changes of isolated spinal cord axons in response to mechanical stretch. Neuroscience 110, 765–777.

Shi, R., Asano, T., Vining, N.C., Blight, A.R., 2000. Control of membrane sealing in injured mammalian spinal cord axons. Journal of Neurophysiology 84, 1763–1769.

Smith, D.H., Wolf, J.A., Lusardi, T.A., Lee, V.M., Meaney, D.F., 1999. High tolerance and delayed elastic response of cultured axons to dynamic stretch injury. Journal of Neuroscience 19, 4263–4269.

Sunderland, S., 1990. The anatomy and physiology of nerve injury. Muscle and Nerve 13, 771–784.

Sunderland, S., Bradley, K.C., 1961. Stress–strain phenomena in human peripheral nerve trunks. Brain 84, 102–119.

Takai, S., Dohno, H., Watanabe, Y., Yoshino, N., Ogura, T., Hirasawa, Y., 2002. In situ strain and stress of nerve conduction blocking in the brachial plexus. Journal of Orthopaedic Research 20, 1311–1314.

Tanelian, D.L., Markin, V.S., 1997. Biophysical and functional consequences of receptor-mediated nerve fiber transformation. Biophysical Journal 72, 1092–1108.

Wall, E.J., Kwan, M.K., Rydevik, B.L., Woo, S.L., Garfin, S.R., 1991. Stress relaxation of a peripheral nerve. Journal of Hand Surgery 16, 859–863.

Wall, E.J., Massie, J.B., Kwan, M.K., Rydevik, B.L., Myers, R.R., Garfin, S.R., 1992. Experimental stretch neuropathy. Changes in nerve conduction under tension. Journal of Bone and Joint Surgery-British 74, 126–129.